Turkish Journal of Electrical Engineering & Computer Sciences

http://journals.tubitak.gov.tr/elektrik/

Research Article

Turk J Elec Eng & Comp Sci
(2021) 29: 1383 – 1400

doi:10.3906/elk-2006-165

The effect of demand response control on stability delay margins of load frequency control systems with communication time-delays

Deniz KATİPOĞLU[1], **Şahin SÖNMEZ**[2,*], **Saffet AYASUN**[3], **Ausnain NAVEED**[4]
[1]Department of Electrical and Electronics Engineering, Faculty of Engineering, Aksaray University, Aksaray, Turkey
[2]Department of Electronics and Automation, Yeşilyurt Vocational High School,
Malatya Turgut Özal University, Malatya, Turkey
[3]Department of Electrical and Electronics Engineering, Faculty of Engineering, Gazi University, Ankara, Turkey
[4]Department of Electrical and Electronics Engineering, Faculty of Engineering,
Niğde Ömer Halisdemir University, Niğde, Turkey

Received: 30.06.2020 • **Accepted/Published Online:** 19.10.2020 • **Final Version:** 31.05.2021

Abstract: This paper studies the effect of dynamic demand response (DR) control on stability delay margins of load frequency control (LFC) systems including communication time-delays. A DR control loop is included in each control area, called as LFC-DR system and Rekasius substitution is utilized to identify stability margins for various proportional-integral (PI) gains and participation ratios of the secondary and DR control loops. The purpose of Rekasius substitution technique is to obtain purely complex roots on the imaginary axis of the time-delayed LFC-DR system. This substitution first converts the characteristic equation of the LFC-DR system including delay-dependent exponential terms into an ordinary polynomial. Then the well-known Routh–Hurwitz stability method is applied to find those imaginary roots and the corresponding stability delay margin known as maximal time-delay. Delay margin results indicate that the inclusion of DR control loop significantly increases stability delay margin and improves the frequency dynamic behavior of the LFC system including time-delays. Theoretical stability margins are confirmed by a proven algorithm, quasi-polynomial mapping-based root finder (QPmR) algorithm and time-domain simulations.

Key words: Frequency regulation, demand response control, Rekasius substitution, stability delay margins

1. Introduction

The objective of load frequency control (LFC) systems is to regulate the frequency around the nominal value and to maintain scheduled power exchanges of the tie-line connecting control areas. The frequency regulation is achieved by adjusting power outputs of conventional thermal or hydro power plants [1]. It is expected that renewable energy (RE) sources including photovoltaic (PV) and wind power systems will have significant share of power generation in the smart power grid prospect[1] [2]. Because of this penetration, the frequency regulation is becoming a difficult task as conventional LFC systems get more complex in terms of frequency regulation. Additionally, highly variable generation of RE sources is inadequate to regulate the system frequency.

Energy storage devices such as electric vehicles (EVs) [3–5] and responsive loads for dynamic demand control [6–9] are becoming promising tools for the frequency control and power grids stability because of short-

*Correspondence: ssonmeztr@gmail.com

[1]U.S. Department of Energy Smart Grid. Grid Modernization and the Smart Grid [online]. Website: http://energy.gov/oe/technology-development/smart-grid/ [accessed 15 March 2020].

comings of RE sources including high costs, low efficiency, and intermittent nature of their power generations. Due to high cost of storage systems, real-time smart active participation of controllable loads known as demand response (DR) has become an essential tool for proper balancing between generation and peak load demand. Thermostatically controlled loads such as heating, ventilation and air-conditioners (HVAC), electric water heaters, fridges, freezers, and vehicle to grid services that have fast response are some examples of these controllable loads. This concept first was introduced by [10] in 1980, responding to the need for seeking a faster and more reliable method than the traditional ones, to maintain balance between generation side and demand side. DR refers to the changes in the electricity usage by demand-side resources from their regular consumption patterns. DR programs are driven by the reasons of network resiliency and economy and, therefore, are broadly categorized into two categories: incentive-based (or dispatchable) programs and time-based (nondispatchable) programs. In the modern smart grid era, DR offers diverse services. It can be used to financially incentivize the utility companies and the customers [11], neutralize the impacts of intermittency of RE sources [12–14], provide ancillary services and mitigate the voltage and frequency fluctuations [15–19], and has several other various purposes such as transmission expansion planning [20] and improved transformer utilization [21].

The DR control is a useful compensation for conventional power system frequency regulation approaches due to its fast response, flexibility and economic efficiency. Therefore, there exists several studies devoted to investigate the impact of DR on the frequency regulation for the conventional LFC and automatic generation control (AGC) schemes. In [22], a DR control loop having communication time-delay was first introduced to the traditional single-area LFC model. Results presented in that study clearly illustrated that LFC systems enhanced by a DR control loop (LFC-DR) have a superior dynamic performance compared to the performance of the conventional LFC. In [23], the DR control loop with communication time-delay was implemented into each control area of a two-area thermal LFC system and the cooperative control action via LFC and DR loops was shown to be sufficient to guarantee minimum frequency deviation profile. In order to quickly stabilize the frequency of different control areas, the tie-line power was adopted as the additional input signal of DR control loop and genetic algorithm was used to determine optimal controller gains [18]. Using H_∞ performance analysis and the Particle Swarm Optimization algorithm, a robust proportional-integral-derivative (PID)-type controller for a multiarea LFC-DR system in a deregulated multiarea power system was proposed in [24] to design a PID load frequency controller providing the robustness to the load disturbances, parameter uncertainties, and multiple delays in the secondary and DR control loops. In [25], a single-area LFC system was modified by adding both DR and virtual inertia control loops with associated communication time-delays in order to improve frequency dynamics and the impact of various parameters of DR and virtual control loops such as time-delays, their power sharing factors and frequency dead band was comprehensively analyzed. An intelligent DR scheme was presented in [12] to determine the control area where the disturbances occurred and to apply the DR exactly to that control area. Additionally, a fuzzy-PI-based supervisory controller was proposed as a coordinator between the demand response and secondary frequency control avoiding large frequency overshoots/undershoots caused by the communication delays. In [15], for primary and secondary frequency regulation, a thermostatic load control strategy using heating, ventilation, and air-conditioning units and electric water heaters was proposed. It was shown that a relatively stable frequency reserve could be provided by considering daily demand profile of thermostatic loads. In [26], in order to decrease frequency detection error and communication delay, a hybrid control approach was developed as a combination of centralized and distributed control methods used to control the flexible loads. By considering the load disturbances and uncertainties in system parameters, [27]

proposed active disturbance rejection control to increase the frequency robustness and designed an adaptive delay compensator to decrease the impact of communication delays on the frequency stability for single-area LFC system with DR control loop. Recently, authors in [28] extended their earlier work reported in [25] in order to develop a mathematical model for sensitivity and stability analysis of the system frequency response with respect to important parameters associated with DR and virtual control loops. Results presented in that work revealed that the performance as well as the stability of the closed-loop system is sensitive to changes in the share of supplementary, DR, and virtual inertia controls. Finally, in [19], an intelligent DR control loop with communication delay was implemented to a single area thermal power system integrated with a wind power generation system and linear matrix inequality with linear quadratic regulator controller was proposed as a coordinator between the DR loop and secondary control loop to minimize the frequency deviation caused by communication delays.

Communication time-delays have become a great concern in the dynamic performance of traditional LFC systems since such time-delays reduce the control system damping performance and even could cause instability if delays exceed the upper bound or delay margin for stability [29–31]. Time-delays are experienced in LFC systems because of an open and distributed communication network used to transmit measured data from power plant to central controller or vice versa. With the increasing integration of RE sources, EVs, and DR control, such delays have even become much more significant [22–25, 32–35]. Even though there exist various studies on the delay-dependent stability and the delay margin computation of the conventional LFC systems, studies focusing on the impact of both time-delays and the integration of DR control on the frequency regulation are very limited. For example, studies reported in [22, 23, 25, 28] recognized the importance of time-delays observed in the DR control loop on the frequency regulation. However, time-delays in the secondary control loop was neglected. It is well known in the literature that communication delay in the secondary loop is larger than one in the DR control loop, which in turns significantly affects the frequency stability [29–31]. Moreover, those studies utilized an approximate approach for the exponential type transfer function of the time-delay in the DR control loop. Such an approximation does not reflect the true characteristic of time-delays and their impact on the stability and, additionally, increases the system dimension depending on the order used in the Padé approximation. More importantly, the exact computation of stability delay margins of LFC-DR systems and analytical studies on the impact of DR control loop on stability delay margins were not presented. Similarly, in [24], stability delay margins were obtained by trial and error simulation method rather than using an exact method. In [26, 27], various compensation schemes were proposed to decrease the frequency deviation in the presence of time-delays in the DR control loop. In those studies, authors did not present any qualitative/quantitative analysis to determine the impact of the DR controls with time-delays on the delay-dependent stability of LFC-DR systems.

To overcome shortcomings of existing studies on the time-delayed LFC-DR systems, this paper aims to compute stability delay margins of LFC-DR systems with time-delay on the secondary control loop. In the existing literature, various approaches are presented to determine stability delay margins of LFC systems with time-delay. These might be classified as frequency-domain direct methods and time-domain indirect approaches. The former group of methods aims to calculate complex roots on the imaginary axis of the quasi-characteristic polynomial. This group of approaches includes: i) direct method based on elimination of exponential terms [36], ii) Rekasius substitution [37–39], iii) frequency sweeping test [33]. Among these methods, the direct method of Walton and Marshall [36] was effectively implemented to determine delay margins of time-delayed two-area LFC systems and microgrid not including DR control loop [29, 40] and single-area LFC system with

EVs aggregator [35]. The Rekasius substitution was applied to delay margin computation of microgrid LFC system [41], two-area LFC system not having DR control loop [42] and single-area LFC system with EVs aggregator [34]. The frequency sweeping test was applied to the delay margin computation of a single-area LFC system with EVs aggregator [33]. The existing studies clearly show that the frequency-domain direct methods accurately determine stability delay margins of electrical power systems with communication time-delays. However, the main disadvantage of these methods is that they can be used for only constant delay cases. A detailed literature review on the methods for delay margin estimation of linear time-invariant continuous-time systems with constant delays can be found in a survey of Pekař and Gao [43]. Both the direct method and Rekasius substitution aim to eliminate the delay-dependent transcendental (exponential) terms in the quasi-characteristic polynomials using different approaches. The direct method employs a recursive procedure without using any approximation and obtains a regular polynomial without exponential terms whose positive real roots exactly match to the complex roots on the imaginary axis of the original quasi-polynomial [29, 36]. On the other hand, Rekasius substitution is an exact transformation for the roots lying on the imaginary axis. Therefore, these purely complex roots of the characteristic equation with delay-dependent exponential terms are preserved with this substitution. Using this substitution, the system characteristic equation having exponential terms is converted to an ordinary single-variable equation not including any exponential terms. Rekasius substitution enables us to transform the computation problem of delay margin values to the computation of purely imaginary roots of a single-variable regular polynomial having no delay-dependent exponential terms. Routh stability criterion then could be easily used to compute these roots and the corresponding delay margins [37–39]. As explained in details in Section 3, the degree of the augmented characteristic equation without exponential terms obtained by Rekasius substitution is significantly lower than that of the direct method. From the computational point of view, such a reduction in the order of the polynomial while eliminating exponential terms in the quasi-polynomial is a noteworthy advantage of Rekasius substitution when applied to multiarea LFC-DR systems. A detailed comparison of these methods as applied to the two-area LFC system were presented in [42]. Finally, the frequency sweeping test consisting of combination of the binary iteration algorithm and frequency sweeping also computes exact delay margin results. However, the selection of the frequency range for the sweeping test requires undesired computational effort [33].

The time-domain indirect methods are based on Lyapunov stability theory and linear matrix inequalities. These methods can only determine the sufficient conditions for the system stability and there exist various studies focusing on the reduction of its conservativeness [30, 31]. Numerous inequalities were proposed in recent years such as Jensen inequality, Wirtinger inequality [44] free-matrix based inequality [45] and Bessel–Legendre inequality [46]. Time-domain indirect methods were used in stability delay margin computation of multiarea LFC systems without DR control loops [30, 31]. These approaches can be used for both constant and time-varying delay cases. Although there exist tremendous efforts in order to reduce the conservativeness of this approach, it is well-known in the literature that frequency-domain direct methods give more accurate and less conservative stability delay margins than time-domain indirect methods [29–31].

Motivated by our previous studies [34, 41, 42], this paper proposes Rekasius substitution approach to compute stability delay margins of a two-area LFC-DR system. The main contents and contributions of this paper are as follows: Firstly, for the selected power sharing factors between the generators and DR control loop, delay margins are computed for a wide-range of PI controller gains to evaluate the impact of the controller gains. Secondly, delay margins are determined for various power sharing scenarios between the conventional generator and DR control loop to assess how the participation of controllable responsive loads affects stability delay

margins. Thirdly, some case studies for the effectiveness of the proposed method and relationship between participation ratio and delay margin are presented. To the best of authors' knowledge, this paper is the first study on the delay margin computation of multiarea LFC-DR systems. The implementation of an exact analytical method to delay margin computation of LFC-DR system and a comprehensive analysis of the impact of the DR control loop on the stability delay margin and on the frequency regulation are the major contributions of this study. Finally, an independent algorithm known as quasi-polynomial mapping-based root finder (QPmR) algorithm [47, 48] along with time-domain simulations [2] are used to validate the correctness of stability margin results. The comparison of stability delay margins of LFC-DR system with those of LFC system not including DR control loop clearly illustrates that delay margins significantly increase as the participation of the DR control loop into the frequency regulation increases. More importantly, simulation studies prove that the inclusion of the DR control loop reduces undesired oscillations on the frequency response and stabilizes the LFC system including time-delays.

2. Two-area LFC-DR system model

The schematic model of the two-area LFC system with a DR control loop in each control area is presented in Figure 1. Please note that the classic two-area LFC system is illustrated by solid lines while the DR loop in each control area is shown by dashed lines. In this figure, Δf_i, ΔX_{gi}, ΔP_{mi}, ΔP_{gi},ΔP_{DRi} and ΔP_{Li} $(i = 1, 2)$ denote the deviation in the frequency, position of valve, mechanical power output, power output of generator, DR control loop power output and load disturbance in each control area, respectively. Moreover, M_i, D_i, R_i, T_{gi}, T_{ci}, F_{Pi}, T_{ri}, β_i, ACE_i and T_{12} $(i = 1, 2)$ represent the inertia constant, load damping constant, speed regulation constant, time constant of governor, reheat time constant, fraction of total turbine power, turbine time constant, frequency bias factor, area control error, and the tie-line coefficient of each control area respectively. For clarity in presentation, a detailed nomenclature is also given in Appendix.

Please note that a PI controller $G_{ci}(s) = K_{Pi} + \frac{K_{Ii}}{s}$ is used as the LFC controller and DR controller where K_{Pi} and K_{Ii} are the PI controller gains, respectively. With the integration of the DR control into the two-area LFC system, the required the controlling effort denominated as Ω is shared between DR control loop and secondary control loop in each control area. This sharing scheme is given as [22]:

$$\begin{aligned} \Delta P_{Si}(s) &= \alpha_0 \Omega \\ \Delta P_{DRi}(s) &= \alpha_1 \Omega \end{aligned} \tag{1}$$

where α_0 and α_1 represent participation ratio of the secondary and DR control loops with $\alpha_0 + \alpha_1 = 1$, respectively. Finally, the measurement and data transfer time-delays in the secondary control loop are lumped. The delays in each control area are assumed to be equal and they are represented by an exponential function of $e^{-s\tau_1} = e^{-s\tau_2} = e^{-s\tau}$ as depicted in Figure 1.

The characteristic polynomial of the two-area system in Figure 1 needs to be determined to evaluate the DR control loop effect on delay margins and thus, to examine the delay-dependent stability of LFC-DR system. This polynomial is transcendental type and is given as

$$\Delta(s, \tau) = P(s) + Q(s)e^{-\tau s} + R(s)e^{-2\tau s} = 0, \tag{2}$$

[2] MathWorks Inc. (2019). MATLAB [online]. Website https://www.mathworks.com/products/matlab.html [accessed 20 June 2019].

where $P(s)$, $Q(s)$ and $R(s)$ polynomials of s whose coefficients depend on system parameter are determined as

$$\begin{aligned} P(s) &= p_{13}s^{13} + p_{12}s^{12} + p_{11}s^{11} + p_{10}s^{10} + p_9s^9 + p_8s^8 + p_7s^7 + p_6s^6 + p_5s^5 + p_4s^4 + p_3s^3 \\ Q(s) &= q_{10}s^{10} + q_9s^9 + q_8s^8 + q_7s^7 + q_6s^6 + q_5s^5 + q_4s^4 + q_3s^3 + q_2s^2 \\ R(s) &= r_7s^7 + r_6s^6 + r_5s^5 + r_4s^4 + r_3s^3 + r_2s^2. \end{aligned} \tag{3}$$

It must be stated that the inherent nonlinearities in power system such as generation rate constraints, governor dead band and rate limiter in the DR control loop are not taken into account in this paper. In the delay-dependent stability analysis of LFC systems, such nonlinearities are neglected and a linear time-invariant model is commonly used due to the small disturbances in the system [16, 29–33].

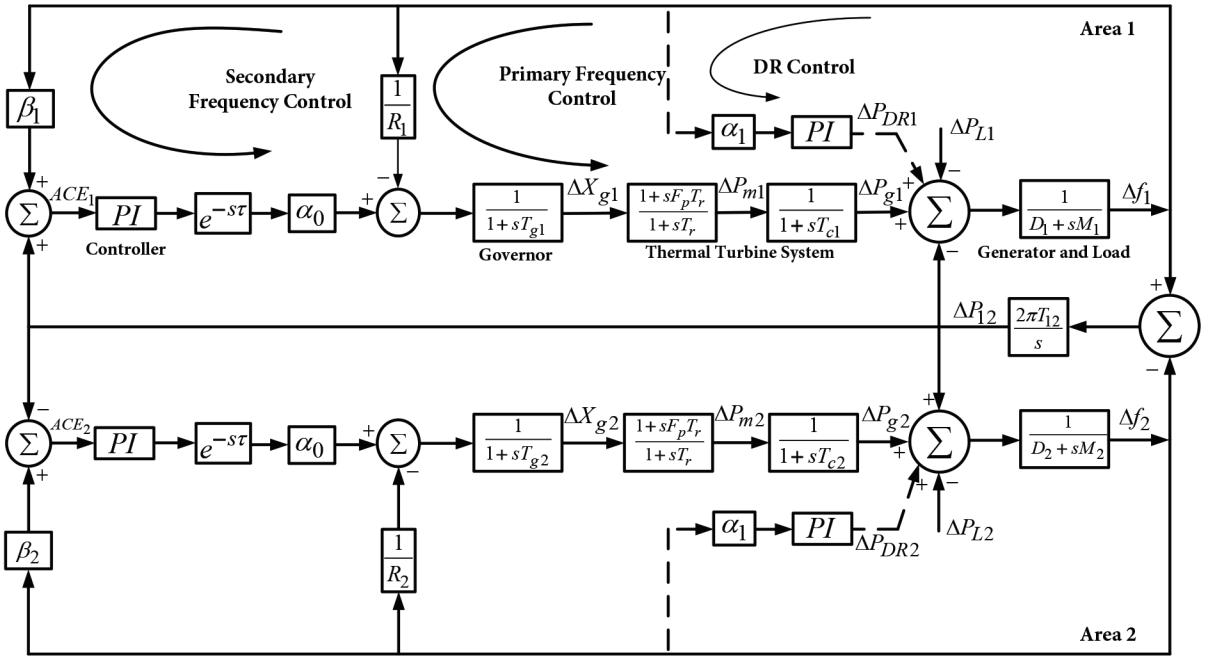

Figure 1. The schematic diagram of two-area LFC system with DR loop.

3. Stability margin identification: Rekasius substitution

The main purpose of stability analysis of time-delayed dynamical system is to determine that if the system is delay-dependent stable or delay-independent stable. If the system is delay-independent stable, this implies that the system remains stable for all finite delays. If the system is delay-dependent stable, this implies that the system is stable for $\tau < \tau^*$ and unstable for $\tau > \tau^*$ where τ^* represents the stability delay margin for selected system parameters.

For the LFC-DR system whose characteristic equation is given in (2) to be stable, all roots of this equation have to be located in the stable left half of the $s-$ plane. It should be noticed that the characteristic polynomial of the LFC-DR system in (2) is a quasi-polynomial because of exponential terms $e^{-\tau s}$ and $e^{-2\tau s}$. The quasi-polynomials have infinite many roots and calculation of these roots is quite hard. Therefore, the main idea is to find time-delay for which the quasi-polynomial has roots located on imaginary axis. A substitution suggested

by Rekasius [37] is defined below for the exponential term to overcome this issue [37–39]:

$$e^{-\tau s} = \frac{1 - Ts}{1 + Ts} \quad \tau \in \Re^{+}, \quad T \in \Re \tag{4}$$

This substitution is used only for $s = j\omega_c$ and presents an exact solution for roots on the $j\omega-$ axis. Furthermore, substitution of $s = j\omega_c$ into (4), the following mapping condition connecting $j\omega_c$ and T is obtained [37–39]:

$$\tau* = \frac{2}{\omega_c}\left[Tan^{-1}(\omega_c T) \pm \ell\pi\right] \quad \ell = 0, 1, 2, ... \tag{5}$$

In order to eliminate exponential terms in (2), Rekasius substitution in (4) needs to be utilized as follows:

$$\Delta(s,\tau) = P(s) + Q(s)\left(\frac{1 - Ts}{1 + Ts}\right) + R(s)\left(\frac{1 - Ts}{1 + Ts}\right)^2 = 0\,. \tag{6}$$

After some simplifications, the augmented characteristic polynomial of LFC-DR system is expressed in a simpler form as

$$\begin{aligned}\Delta(s,T) = {} & b_{15}s^{15} + b_{14}s^{14} + b_{13}s^{13} + b_{12}s^{12} + b_{11}s^{11} + b_{10}s^{10} + \\ & b_9 s^9 + b_8 s^8 + b_7 s^7 + b_6 s^6 + b_5 s^5 + b_4 s^4 + b_3 s^3 + b_2 s^2 = 0.\end{aligned} \tag{7}$$

The coefficients of (7) are given in Appendix.

It should be noted that Rekasius substitution transforms the stability problem effectively to the computation of complex roots of a single-variable polynomial of (7) on the $j\omega-$ axis. It is clear from (7) that Rekasius substitution converts the quasi-polynomial of LFC-DR system in (2) to a regular polynomial whose coefficients depend on T only. Where $T \in \Re$, and unknown T variables could be positive or negative. With Rekasius substitution, the 13^{th} order quasi-polynomial with delay terms is now transformed into a 15^{th} order polynomial given in (7) without any exponential terms. Moreover, Rekasius substitution preserves complex roots on the imaginary axis, indicating that $\Delta(s,\tau) = 0$ and $\Delta(s,T) = 0$ have the same complex roots on the $j\omega-$ axis and there is no relation between the remaining real or complex roots. Since, the two equations have the same complex roots on $j\omega-$ axis, such roots of $\{(T,\omega_c)$ for $\Delta(s,T) = 0\}$ instead of $\{(\tau*,\omega_c)$ for $\Delta(s,\tau) = 0\}$ could be easily determined. The aim is to calculate all $T \in \Re$ values that yield purely imaginary roots, $s = \pm j\omega_c$ of $\Delta(s,T) = 0$. Such T values and the corresponding roots are computed by Routh–Hurwitz criterion. For this purpose, a Routh's array for $\Delta(s,T) = 0$ is formed and the nonzero term $R_{1,1}(T)$ in the s^1 row is set to zero [37–39]. The Routh's array is given as follows:

$$\begin{array}{ccccccccc}
s^{15} & b_{15} & b_{13} & b_{11} & b_9 & b_7 & b_5 & b_3 \\
s^{12} & b_{14} & b_{12} & b_{10} & b_8 & b_6 & b_4 & b_2 \\
s^{11} & R_{11,1}(T) & R_{11,2}(T) & R_{11,3}(T) & R_{11,4} & R_{11,5}(T) & R_{11,6}(T) & 0 \\
\vdots & \vdots & \vdots & \vdots & \vdots & \vdots & \vdots & \vdots \\
\vdots & \vdots & \vdots & \vdots & \vdots & \vdots & \vdots & \vdots \\
s^2 & R_{2,1}(T) & R_{2,2}(T) & 0 & 0 & 0 & 0 & 0 \\
s^1 & R_{1,1}(T) & 0 & 0 & 0 & 0 & 0 & 0 \\
s^0 & R_{0,1}(T) & 0 & 0 & 0 & 0 & 0 & 0
\end{array} \tag{8}$$

The following expression enables us to find elements in the array.

$$R_{i,j}(T) = R_{i+2,j+1}(T) - \frac{R_{i+1,j+1}(T)R_{i+2,1}(T)}{R_{i+1,1}(T)}, \tag{9}$$

where the $ij-$th element of Routh's array is denoted by $R_{i,j}(T)$. As per Routh stability criterion, the unstable roots are given by the number of sign changes (NS) in the first column. It should be observed that all the first column elements depend on T, as a rational function. In order to calculate T values that result in complex roots of (7) on the $j\omega_c-$ axis, the following polynomial is found by setting the only nonzero term in s^1 row to zero

$$R_{1,1}(T) = R_{3,2}(T) - \frac{R_{2,2}(T)R_{3,1}(T)}{R_{2,1}(T)} = t_{22}T^{22} + ... + t_6T^6 + t_5T^5 + ... + t_1T + t_0 = 0. \tag{10}$$

Real roots of (10) are first determined and, the corresponding complex roots of (7) on the $j\omega_c-$ axis is then computed using the following auxiliary equation obtained by s^2 row as:

$$R_{2,1}(T)s^2 + R_{2,2}(T) = 0 \Rightarrow s = \pm j\omega_c = \pm j\sqrt{\frac{R_{2,2}(T)}{R_{2,1}(T)}}. \tag{11}$$

Notice that both $R_{2,1}(T)$ and $R_{2,2}(T)$ terms in (11) depend upon T. In order to have complex roots of (7) on the $j\omega-$ axis, a sign agreement between these terms is required. This sign agreement is defined as $R_{2,1}(T)R_{2,2}(T) > 0$ and a change in the NS occurs at those finite values of T. Note that if (10) does not have any real roots satisfying the sign agreement, then the two-area LFC-DR system will be delay independent stable for the selected system and controller parameters. Suppose that there exists q of such T's $\{T\} = \{T_1, T_2, \cdots, T_k\}$. The characteristic polynomial in (7) will have a pair of imaginary roots $(s = \pm j\omega_c)$ and the quasi-polynomial of (2) at each T_k. For each T's the corresponding crossing frequencies are computed using (11). Let's this set be $\{\omega_c\} = \{\omega_{c1}, \omega_{c2}, \cdots, \omega_{ck}\}$. Finally, stability margins $\{\tau_k^*\}$ for each $\{T_k, \omega_{ck}\}$ are determined by employing (5) and the minimum among those is selected as the stability delay margin of the LFC-DR system.

At this point, it will be useful to compare the Rekasius substitution method with another well-known frequency domain direct method presented by Walton and Marshall [36] that was applied to the delay margin computation of LFC systems with constant communication delays [29]. The direct method is an analytical procedure that converts the transcendental characteristic Equation (2) into a regular polynomial, similar to (7), without the transcendentality by eliminating the highest degree of commensuracy terms successively. For the two-area LF-DR system, the resulting polynomial will have a degree of $n.2^p = (13)2^2 = 52$ ($p = 2$, the degree of commensuracy) and its real solutions give complex roots on the imaginary axis. The proposed method based on Rekasius substitution has two main advantages. The first advantage is that the degree of the augmented polynomial of (7) is $n + p = 13 + 2 = 15$, which is significantly lower than that of the direct method. Moreover, the degree of the polynomial given in (10) used to determine the real values of T is 22, which is again very much lower than that of the direct method. Such a reduction in the order of the polynomials while eliminating commensurate terms in the quasi-polynomials is a noteworthy advantage of Rekasius substitution when applied to the multiarea LFC-DR systems. The second advantage is that we look for the real roots T of (10) only, not complex ones. This is an important advantage as complex roots, especially purely imaginary ones, are quite difficult to find when numerical errors creep in [38, 43].

4. Results

This section gives results for stability delay margins of the LFC-DR system and verification studies of theoretical stability delay margins by QPmR algorithm. System parameters in each area are as follows [32]:

$$M_i = 8.8, D_i = 1, F_{Pi} = 1/6, R_i = 1/11, \beta_i = 21, T_{gi} = 0.2, T_{ci} = 0.3, T_{ri} = 12, T_{12} = 0.1 (i = 1, 2).$$

4.1. Illustration of the computation process for stability delay margins

The delay margin computation process and verification studies consists of eight steps. In the following steps, controller parameter values and participation ratios of the DR and secondary control loops are selected as ($K_P = 0.5,\ K_I = 0.3$) and ($a_0 = 0.6,\ a_1 = 0.4$), respectively.

Step 1: Determine the characteristic polynomial in (2) for selected parameters, participation ratios and PI controller gains. The characteristic equation is given as:

$$\begin{aligned}\Delta(s,\tau) = {} & s^{13} + 17.1s^{12} + 110s^{11} + 333s^{10} + 488s^9 + 353s^8 + 191s^7 + 56.9s^6 + 11.7s^5 + 0.55s^4 + \\ & 0.01s^3 + (3.97s^{10} + 38.5s^9 + 113s^8 + 126s^7 + 74.1s^6 + 26.7s^5 + 5.12s^4 + 0.22s^3 + 0.01s^2)e^{-s\tau} + \\ & (3.95s^7 + 8.93s^6 + 7.67s^5 + 3.03s^4 + 0.51s^3 + 0.02s^2)e^{-2s\tau} = 0.\end{aligned} \tag{12}$$

Step 2: Obtain the resulting equation presented in (7). The coefficients of new polynomial with the 15^{th} order are presented in Appendix.

Step 3: Determine the polynomial of T given in (10) and compute all its real roots. The 22^{nd} order of this polynomial has four real roots given below

$T_1 = 1.429, T_2 = 27.683, T_3 = 7.483, T_4 = 35.715$.

Step 4: Find T values that satisfy the sign agreement of $R_{2,1}(T)R_{2,2}(T) > 0$ resulting in purely complex conjugate roots of (7). Among these T values, $T_1 = 1.429$ and $T_3 = 7.483$ are found to satisfy the sign agreement.

Step 5: Compute the purely imaginary roots of (7) using (11) for $T_1 = 1.429$ and $T_3 = 7.483$. Those roots are found as $s = \pm j\omega_c = \pm 0.3811 rad/s$ and $s = \pm j\omega_c = \pm 0.1687 rad/s$.

Step 6: Compute stability delay margin for each $\{T, \omega_c\}$ pair given in Step 5 using (5). The stability delay margin for $T_1 = 1.429$ and $\omega_{c1} = 0.3811 rad/s$ is found as $\tau* = 2.6176s$ while it is found as $\tau* = 10.6783s$ for $T_3 = 7.483$ and $\omega_{c3} = 0.1687 rad/s$.

Step 7: Choose the lowest value found in Step 6 as the delay margin or maximal delay value of the two-area LFC-DR system; that is, $\tau* = 2.6176s$ with a root crossing of $\omega_{c1} = 0.3811 rad/s$.

Step 8: Verify the accuracy of the root crossing and stability delay margin found in Step 7.

The accuracy of the theoretical delay margin ($\tau*$) and root crossing ($\pm j\omega_c$) found in Step 7 is verified by QPmR algorithm and time-domain simulation. For verification purposes, the system data given before, the PI gains of ($K_p = 0.5, K_I = 0.3$) and the participation ratios of ($\alpha_0 = 0.6, \alpha_1 = 0.4$) are used. For time-domain simulations, a step load disturbances of $\Delta P_{d1} = 0.2\ pu$, $\Delta P_{d2} = 0$ at $t = 0$ is considered in the control area 1 and the root location of the characteristic Equation (2) by the QPmR algorithm and frequency deviation responses by Matlab/Simulink are obtained. Recall that the stability delay margin for the selected parameters is determined as $\tau* = 2.6176s$ in Step 7. Figure 2 shows the location of influential roots of the characteristic polynomial and the frequency response of the control area 1 around the stability delay margin, namely for $\tau = 2.5176s$, $\tau* = 2.6176s$ and $\tau = 2.7176s$. Figure 2a shows these roots and the frequency deviation for $\tau = 2.5176s$, which is less than the delay margin, $\tau* = 2.6176s$. It is obvious that all roots of

characteristic polynomial in (1) are in the stable left half of the $s-$plane and oscillations in the frequency are decaying. Therefore, the LFC-DR system is stable. For $\tau* = 2.6176s$, a pair of complex roots is now on the imaginary axis as depicted in Figure 2b, and the frequency deviation of the control area 1 has the sustained oscillations, indicating the marginal stability. Note that QPmR algorithm gives the same purely imaginary roots of $s = \pm j\omega_c = \pm 0.3811 rad/s$ as the one obtained by the proposed method in Step 5. Finally, for $\tau = 2.7176s$, a pair of complex roots crosses the imaginary axis towards the unstable right half plane, which causes unstable growing oscillations in the frequency deviation as illustrated in Figure 2c.

4.2. The effect of participation ratios and controller parameters on stability delay margins

Stability margins are determined for various PI controller gains and participation ratios. Stability delay margins are given in Tables 1–3 for $(\alpha_0 = 1, \alpha_1 = 0)$, $(\alpha_0 = 0.8, \alpha_1 = 0.2)$ and $(\alpha_0 = 0.6, \alpha_1 = 0.4)$, respectively. For all cases, stability delay margins decrease as K_I increases for the fixed K_P indicating a less stable LFC-DR system. On the other hand, as K_P increases, stability delay margins increases for almost all values of K_I, resulting in a more stable LFC-DR system. It must be mentioned here that stability delay margins are not computed in some values of K_I and K_P when the delay-free LFC-DR system $(\tau = 0)$ is unstable. The corresponding positions are labeled as (*) in Tables.

Table 1. Stability delay margins for $\alpha_0 = 1, \alpha_1 = 0$.

$\tau*(s)$	K_I				
K_P	0.1	**0.3**	0.5	0.7	0.9
0.1	6.0291	0.4517	*	*	*
0.3	5.3667	0.9471	0.2353	*	*
0.5	3.4518	**1.2321**	0.5146	0.1846	0.0012
0.7	2.1069	1.2551	0.7093	0.3711	0.1671
0.9	1.6669	1.1649	0.7658	0.4846	0.2882

Table 2. Stability delay margins for $\alpha_0 = 0.8, \alpha_1 = 0.2$.

$\tau*(s)$	K_I				
K_P	0.1	**0.3**	0.5	0.7	0.9
0.1	9.1909	0.8820	0.0844	*	*
0.3	9.5614	1.3873	0.4510	0.0922	*
0.5	5.9953	**1.6679**	0.7410	0.3338	0.1108
0.7	3.4560	1.7608	0.9460	0.5305	0.2858
0.9	2.3151	1.5812	1.0384	0.6780	0.4303

More importantly, the comparison of delay margins in Tables 2 and 3 with ones in Table 1 clearly reveals the fact that stability delay margins significantly increase when a DR control loop with a corresponding participation ratio is included in LFC system for frequency regulation. For example, one can see from Table 1 that for $K_P = 0.5, K_I = 0.3$, stability margin is determined as $\tau* = 1.2321s$ when the LFC system does not include a DR loop. This case corresponds to an operation scenario that all control effort for frequency regulation is provided by the secondary control loop $(\alpha_0 = 1, \alpha_1 = 0)$. When the participation of the secondary

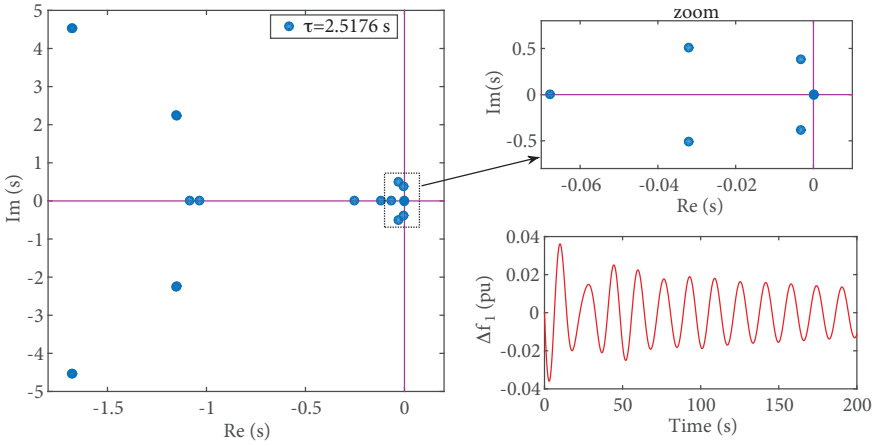

(a) Stable case (τ = 2.5176s)

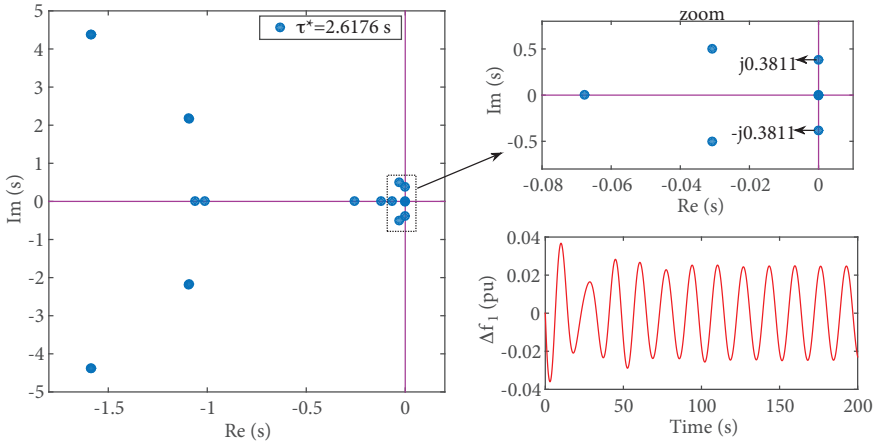

(b) Marginally stable case (τ = 2.6176s)

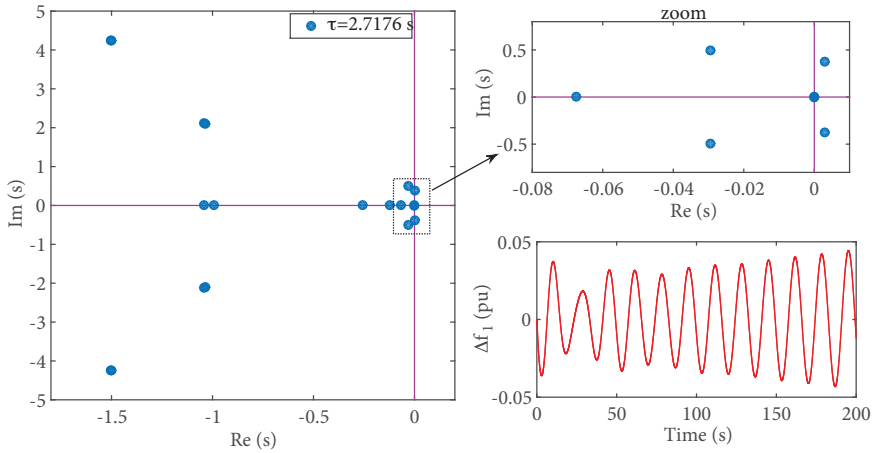

(c) Unstable case (τ = 2.7176s)

Figure 2. Dominant roots distribution and frequency responses.

Table 3. Stability delay margins for $\alpha_0 = 0.6, \alpha_1 = 0.4$.

$\tau*(s)$	K_I				
K_P	0.1	**0.3**	0.5	0.7	0.9
0.1	14.0744	1.8308	0.4898	0.0670	*
0.3	15.2433	2.3583	0.8827	0.3663	0.1076
0.5	15.0565	**2.6177**	1.1900	0.6252	0.3249
0.7	11.6460	2.6595	1.4076	0.8372	0.5140
0.9	4.9916	2.5691	1.5427	1.0010	0.6724

control loop is reduced to 80% [20% participation of the DR control loop $(\alpha_0 = 0.8, \alpha_1 = 0.2)$], the stability delay margin increases from $\tau* = 1.2321s$ to $\tau* = 1.6679s$ which illustrates 35.37% increase. Furthermore, the control effort of the secondary control loop is reduced to 60% of the total control effort (or 40% participation of the DR control loop, $(\alpha_0 = 0.6, \alpha_1 = 0.4)$), the stability delay margin rises to $\tau* = 2.6177s$, which corresponds to 112.456% increase with respect to the case not including DR control loop. More importantly, it must be noted that for some PI controller gains (for example $K_P = 0.5$ and $K_I = 0.3$ or 0.9), the LFC system not including DR is found to be unstable (Table 1). With the inclusion of the DR control loop with a participation ratio of $\alpha_1 = 0.4$, the LFC system becomes delay-dependent stable with certain amount of delay margins (Table 3). Such results clearly indicate that the stability of the traditional LFC systems is significantly improved when a DR control loop is added.

4.3. The effect of DR control loop on the frequency responses

In this section, the stabilizing effect of the participation of the DR control loop on the frequency stability of the LFC-DR system with time-delay is broadly investigated. It is evident from Tables 2 and 3 that the integration of the DR control loop into the LFC system increases stability delay margin values and thus, expands the stability margin when Table 1 is compared with Tables 2 and 3. In order to indicate the effect of DR control loop on the LFC system stability, PI controller parameters are chosen as $K_I = 0.3, K_P = 0.5$ and the delay margin value corresponding to the controller gains is computed as $\tau* = 1.2321s$ from Table 1 when the DR control loop is not considered. The contribution of DR control participation is investigated for the three time-delay values $(\tau = 1s < \tau* = 1.2321s < \tau = 1.3s)$ selected around the delay margin $(\tau* = 1.2321s)$ when participation ratios of the secondary and DR control loops are chosen as $(\alpha_0 = 1, \alpha_1 = 0)$, $(\alpha_0 = 0.8, \alpha_1 = 0.2)$ and $(\alpha_0 = 0.6, \alpha_1 = 0.4)$. For three different cases, the frequency responses of the control area 1 are simulated under disturbances of $\Delta P_{d1} = 0.2\ pu$ and $\Delta P_{d2} = 0$ at $t = 0$ in Figures 3-5. In these figures, the frequency responses for $(\alpha_0 = 1, \alpha_1 = 0)$, $(\alpha_0 = 0.8, \alpha_1 = 0.2)$ and $(\alpha_0 = 0.6, \alpha_1 = 0.4)$ are shown by using cyan, red and magenta colors, respectively. In the first case, the delay value is chosen as $\tau = 1.0s$ and at first, DR loop is not included, $(\alpha_0 = 1, \alpha_1 = 0)$. Please note from Table 1 that this case is stable case as the selected delay is less than the stability delay margin, $(\tau = 1.0s < \tau* = 1.2321s)$. The system frequency response for this case is shown in Figure 3. It is clear that the frequency response has undesired oscillations even though it is stable. Next, the participation ratios of the secondary control loop and the DR control loop is selected as $(\alpha_0 = 0.8, \alpha_1 = 0.2)$ and $(\alpha_0 = 0.6, \alpha_1 = 0.4)$. Figure 3 also compares the frequency response with that of LFC system not including DR loop. It is evident from Figure 3 that undesired oscillations are readily damped

when 20% or 40% of the control effort is provided by the DR control loop. This case clearly illustrates that the inclusion of DR control loop significantly improves the frequency response performance of the LFC system. In the second case, time-delay is selected as $\tau* = 1.2321s$ such that the time-delayed LFC system not including DR control loop is marginally stable as presented in Table 1. Figure 4 compares the frequency responses for the same participation ratios of the first case. It is clear that with the inclusion of the DR control loop, the marginally stable LFC system becomes stable. In the third case, delay value is chosen as $\tau = 1.3s$ for which LFC system not including DR control loop is unstable since this delay is larger than the stability delay margin of $\tau* = 1.2321s$. Figure 5 clearly shows that the inclusion of DR control loop with a participation ratio of 20% or 40% makes a stable LFC system. The second and third cases clearly illustrates the stabilizing effect of DR control loop for LFC system in the presence of communication time-delay.

Finally, the impact of the participation ratio of the DR control on the stability delay margin is analyzed for three different PI controller gains, namely $(K_P = 0.5, K_I = 0.3)$, $(K_P = 0.5, K_I = 0.5)$ and $(K_P = 0.5, K_I = 0.7)$. Figure 6 depicts that the stability delay margin remarkably increases for all controller gain values when participation ratio of the DR control loop is changed from $\alpha_1 = 0$ (DR not included) to $\alpha_1 = 0.5$ (50% participation of the DR control loop).

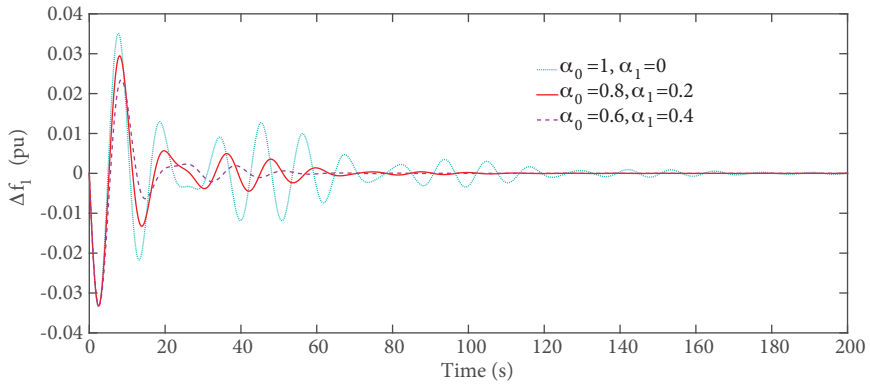

Figure 3. The effect of DR loop on the frequency response for $\tau = 1s$.

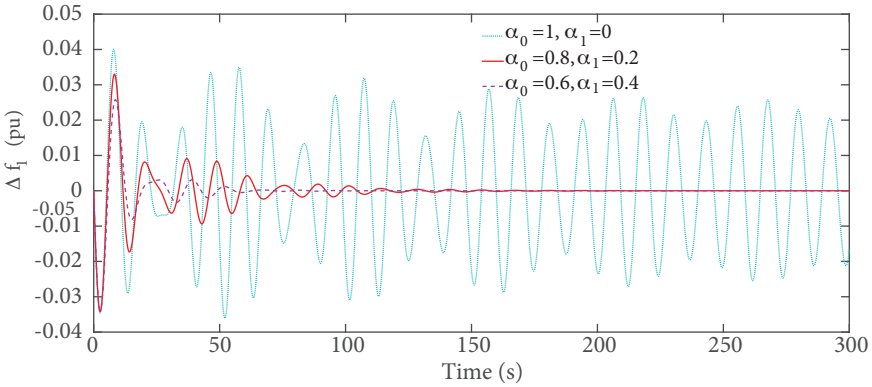

Figure 4. The stabilizing effect of DR loop on the frequency response for $\tau = 1.2321s$.

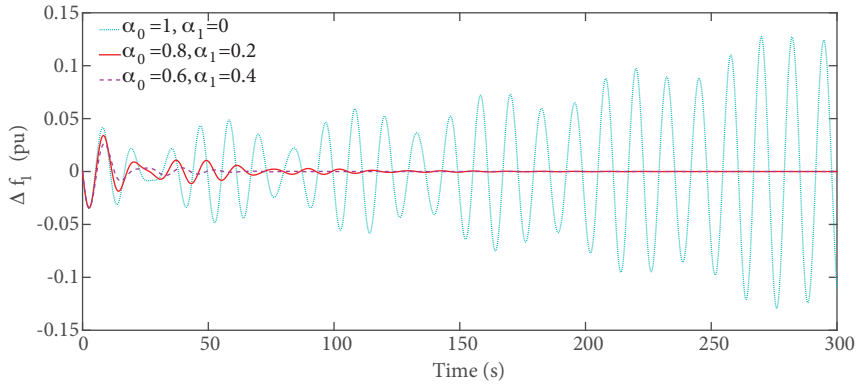

Figure 5. The stabilizing effect of DR loop on the frequency response for $\tau = 1.3s$.

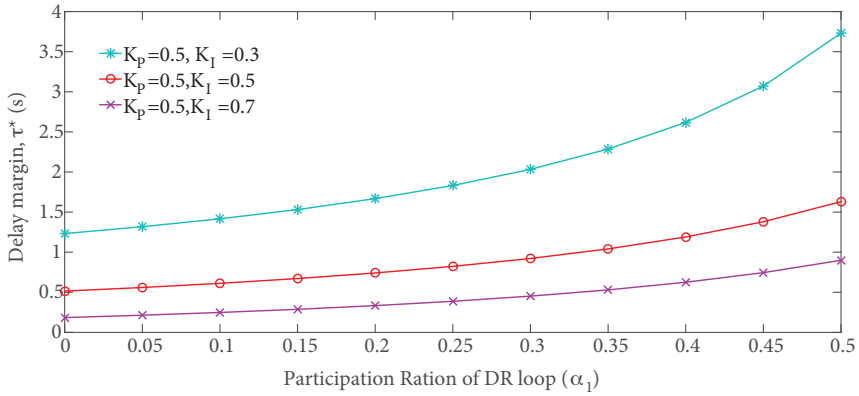

Figure 6. The effect of the participation ratio of the DR loop on the stability delay margin.

5. Conclusion

This paper has focused on an extensive examination of the impact of DR control loop on the stability delay margin of the two-area LFC systems having communication time-delays in the secondary control loop. A frequency-domain Rekasius substitution technique is used to determine stability margins of the LFC-DR system for a wide range controller gains and different participation ratios of the secondary and DR control loops. Theoretical delay margins have been confirmed by time-domain simulations and the QPmR root finder technique. From the results, the following comments could be made:

- Stability delay margins decrease as the (K_I) controller parameter increases for fixed (K_P) controller parameter, indicating a less stable LFC-DR system.
- Stability delay margins generally increase as the proportional controller gains increases for fixed integral control gain, indicating a more stable LFC-DR system.
- A small percentage increase in the participation of the DR loop on the frequency regulation service of the system causes a remarkable rise in stability delay margins for all (K_P, K_I) controller parameters.
- With the inclusion of the DR control loop, more than 100% increase in the stability delay margin is observed for some PI controller gains.

- The inclusion of the DR control loop significantly reduces undesired oscillations on the system frequency and more importantly stabilizes the LFC system with time-delays.

Evidently, presented results could be utilized to properly select participation ratios and controller gains of the secondary and DR control in order to minimize the frequency deviation. With the proper selection of participation ratios, a desired frequency performance with adequate damping will be guaranteed even if communication delays are observed in the LFC system. As future work, the impact of DR control loop on stability regions in the PI controller parameters space will be investigated for robust PI controller design, and incommensurate time-delays in the secondary and DR control loops will be considered in the delay-dependent stability analysis. As future work, the impact of DR control loop on stability regions in the PI controller parameters space will be investigated for robust PI controller design. Furthermore, incommensurate time-delays for multiarea realistic LFC-DR systems will be considered to investigate the impact of the DR control loop on the stability delay margin using Rekasius substitution together with Dixon resultant and discriminant theory [39, 49] and time-domain indirect methods [30–32].

Acknowledgement

This work was supported by the Scientific and Technological Research Council of Turkey (TÜBİTAK) [Grant number 118E744].

References

[1] Kundur P. Power System Stability and Control. New York, NY, USA: McGraw-Hill, 1994.

[2] Bevrani H, Ghosh A, Ledwich G. Renewable energy sources and frequency regulation: survey and new perspectives. IET Renewable Power Generation 2010; 4 (5): 438-457. doi: 10.1049/iet-rpg.2009.0049

[3] Masuta T, Yokoyama A. Supplementary load frequency control by use of a number of both electric vehicles and heat pump water heaters. IEEE Transactions on Smart Grid 2012; 3 (3): 1253-1262. doi: 10.1109/TSG.2012.2194746

[4] Mu Y, Wu J, Ekanayake J, Jenkins N, Jia H. Primary frequency response from electric vehicles in the Great Britain power system. IEEE Transactions on Smart Grid 2013; 4 (2): 1142-1150. doi: 10.1109/TSG.2012.2220867

[5] David AO, Al-Anbagi I. EVs for frequency regulation: cost benefit analysis in a smart grid environment. IET Electrical Systems in Transportation 2017; 7 (4): 310-317. doi: 10.1049/iet-est.2017.0007

[6] Shoreh MH, Siano P, Shafie-Khah M, Loia V, Catalão JP. A survey of industrial applications of demand response. Electric Power Systems Research 2016; 141: 31-49. doi: 10.1016/j.epsr.2016.07.008

[7] Shi Q, Li F, Hu Q, Wang Z. Dynamic demand control for system frequency regulation: concept, review, algorithm comparison, and future vision. Electric Power Systems Research 2018; 154: 75-87. doi: 10.1016/j.epsr.2017.07.021

[8] Paterakisa NG, Erdinç O, Catalão JPS. An overview of demand response: Key-elements and international experience. Renewable and Sustainable Energy Reviews 2017; 69: 871-891. doi: 10.1016/j.rser.2016.11.167

[9] Wang J, Zhong H, Ma Z, Xia Q, Kang C. Review and prospect of integrated demand response in the multi-energy system. Applied Energy 2017; 202: 772-782. doi: 10.1016/j.apenergy.2017.05.150

[10] Schweppe FC, Tabors RD, Kirtley JL, Outhred HR, Pickel FH et al. Homeostatic utility control. IEEE Transactions on Power Apparatus and Systems 1980; 99 (3):1151-1163. doi: 10.1109/TPAS.1980.319745

[11] Fernández-Blanco R, Arroyo JM, Alguacil N, Guan X. Incorporating price-responsive demand in energy scheduling based on consumer Payment minimization. IEEE Transactions on Smart Grid 2016; 7 (2): 817-826. doi: 10.1109/TSG.2015.2427584

[12] Babahajiani P, Shafiee Q, Bevrani H. Intelligent demand response contribution in frequency control of multi-area power systems. IEEE Transactions on Smart Grid 2018; 9 (2): 1282-1291. doi: 10.1109/TSG.2016.2582804

[13] Villena J, Vigueras-Rodríguez A, Gómez-Lázaro E, Fuentes-Moreno JA, Muñoz-Benavente I et al. An analysis of decentralized demand response as frequency control support under critical wind power oscillations. Energies 2015; 8 (11): 12881-12897. doi: 10.3390/en81112349

[14] Hajibandeh N, Ehsan M, Soleymani S, Shafie-khah M, Catalao JPS. The mutual impact of demand response programs and renewable energies: a survey. Energies 2017; 10 (9): 1353. doi: 10.3390/en10091353

[15] Shi Q, Li F, Liu G, Shi D, Yi Z et al. Thermostatic load control for system frequency regulation considering daily demand profile and progressive recovery. IEEE Transactions on Smart Grid 2019; 10 (6): 6259-6270. doi: 10.1109/TSG.2019.2900724

[16] Muñoz-Benavente I, Hansen AD, Gómez-Lázaro E, García-Sánchez T, Fernández-Guillamón A et al. Impact of combined demand-response and wind power plant participation in frequency control for multi-area power systems. Energies 2019; 12 (9): 1687. doi: 10.3390/en12091687

[17] Beil I, Hiskens I, Backhaus S. Frequency regulation from commercial building HVAC demand response. Proceedings of the IEEE 2016; 104 (4): 745-757. doi: 10.1109/JPROC.2016.2520640

[18] Bao YQ, Li Y, Wang B, Hu M, Chen P. Demand response for frequency control of multi-area power system. Journal of Modern Power Systems and Clean Energy 2017; 5 (1): 20-29. doi: 10.1007/s40565-016-0260-1

[19] Bharti K, Singh VP, Singh SP. Impact of intelligent demand response for load frequency control in smart grid perspective. IETE Journal of Research 2020. doi: 10.1080/03772063.2019.1709570

[20] Zakeri AS, Askarian HA. Transmission expansion planning using TLBO algorithm in the presence of demand response resources. Energies 2017; 10 (9): 1376. doi: 10.3390/en10091376

[21] Humayun M, Degefa MZ, Safdarian A, Lehtonen M. Utilization improvement of transformers using demand response. IEEE Transactions on Power Delivery 2015; 30 (1): 202-210. doi: 10.1109/TPWRD.2014.2325610

[22] Pourmousavi SA, Nehrir MH. Introducing dynamic demand response in the LFC model. IEEE Transactions on Power Systems 2014; 29 (4): 1562-1572. doi: 10.1109/TPWRS.2013.2296696

[23] Singh VP, Samuel P, Kishor N. Impact of demand response for frequency regulation in two-area thermal power system. International Transactions on Electrical Energy Systems 2017; 27 (2): 1-23. doi: 10.1002/etep.2246

[24] Zhu Q, Jiang L, Yao W, Zhang CK, Luo C. Robust load frequency control with dynamic demand response for deregulated power systems considering communication delays. Electric Power Components and Systems 2017; 45 (1): 75-87. doi: 10.1080/15325008.2016.1233300

[25] Zaman MSU, Bukhari SBA, Hazazi KM, Haider ZM, Haider R et al. Frequency response analysis of a single-area power system with a modified LFC model considering demand response and virtual inertia. Energies 2018; 11 (4): 787. doi: 10.3390/en11040787

[26] Hui H, Ding Y, Song Y, Rahman S. Modeling and control of flexible loads for frequency regulation services considering compensation of communication latency and detection error. Applied Energy 2019; 250: 161-174. doi: 10.1016/j.apenergy.2019.04.191

[27] Hosseini SA, Toulabi M, Dobakhshari AS, Ashouri-Zadeh A, Ranjbar AM. Delay compensation of demand response and adaptive disturbance rejection applied to power system frequency control. IEEE Transactions on Power Systems 2020; 35 (3): 2037-2046. doi: 10.1109/TPWRS.2019.2957125

[28] Zaman MSU, Bukhari SBA, Haider R, Khan MO, Baloch S et al. Sensitivity and stability analysis of power system frequency response considering demand response and virtual inertia. IET Generation, Transmission & Distribution 2020; 14 (6): 986-996. doi: 10.1049/iet-gtd.2018.6580

[29] Sönmez Ş, Ayasun S, Nwankpa CO. An exact method for computing delay margin for stability of load frequency control systems with constant communication delays. IEEE Transactions on Power Systems 2016; 31 (1): 370-377. doi: 10.1109/TPWRS.2015.2403865

[30] Jiang L, Yao W, Wu QH, Wen JY, Cheng SJ. Delay-dependent stability for load frequency control with constant and time-varying delays. IEEE Transactions on Power Systems 2012; 27 (2): 932-941. doi: 10.1109/TPWRS.2011.2172821

[31] Jin L, Zhang CK, He Y, Jiang L, Wu M. Delay-dependent stability analysis of multi-area load frequency control with enhanced accuracy and computation efficiency. IEEE Transactions on Power Systems 2019; 34 (5): 3687-3696. doi: 10.1109/TPWRS.2019.2902373

[32] Ko KS, Sung DK. The effect of EV aggregators with time-varying delays on the stability of a load frequency control system. IEEE Transactions on Power Systems 2018; 33 (1): 669-680. doi: 10.1109/TPWRS.2017.2690915

[33] Khalil A, Peng AS. Delay margin computation for load frequency control system with plug-in electric vehicles. International Journal of Power and Energy Systems 2018; 38 (3): 1-17. doi: 10.2316/Journal.203.2018.3.203-0060

[34] Naveed A, Sönmez Ş, Ayasun S. Identification of stability delay margin for load frequency control system with electric vehicles aggregator using Rekasius substitution. In: IEEE 2019 Milan PowerTech; Milan, Italy; 2019. pp. 1-6.

[35] Naveed A, Sönmez Ş, Ayasun S. Impact of electric vehicle aggregator with communication time delay on stability regions and stability delay margins in load frequency control system. Journal of Modern Power Systems and Clean Energy 2020. doi: 10.35833/MPCE.2019.000244

[36] Walton KE, Marshall JE. Direct method for TDS stability analysis. IEE Proceedings D - Control Theory and Applications 1987; 134 (2): 101-107. doi: 10.1049/ip-d.1987.0018

[37] Rekasius ZV. A stability test for systems with delays. In: Joint Automatic Control Conference; San Francisco, CA, USA; 1980.

[38] Olgac N, Sipahi R. An exact method for the stability analysis of time-delayed linear time-invariant (LTI) systems. IEEE Transactions on Automatic Control 2002; 47 (5): 793-797. doi: 10.1109/TAC.2002.1000275

[39] Delice I, Sipahi R. Delay-independent stability test for systems with multiple time-delays. IEEE Transactions on Automatic Control 2012; 57 (4): 963-972. doi: 10.1109/TAC.2011.2168992

[40] Gündüz H, Sönmez Ş, Ayasun S. Comprehensive gain and phase margins based stability analysis of micro-grid frequency control system with constant communication time delay. IET Generation Transmission & Distribution 2017; 11 (3): 719-729. doi: 10.1049/iet-gtd.2016.0644

[41] Gündüz H, Sönmez Ş, Ayasun S. Gain and phase margins based stability analysis of micro grid systems with time delay by using Rekasius substitution. Journal of the Faculty of Engineering and Architecture of Gazi University 2019; 34 (1): 553-567 (in Turkish with an abstract in English). doi: 10.17341/gazimmfd.416515

[42] Sönmez Ş, Ayasun S. Gain and phase margins-based delay margin computation of load frequency control systems using Rekasius substitution. Transactions of the Institute of Measurement and Control 2019; 41 (12): 3385-3395. doi: 10.1177/0142331219826653

[43] Pekař L, Gao Q. Spectrum analysis of LTI continuous-time systems with constant delays: a literature overview of some recent results. IEEE Access 2018; 6: 35457-35491. doi: 10.1109/ACCESS.2018.2851453

[44] Seuret A, Gouaisbaut F. Wirtinger-based integral inequality: Application to time-delay systems. Automatica 2013; 49 (9): 2860-2866. doi: 10.1016/j.automatica.2013.05.030

[45] Zeng HB, Liu, Wang W. A generalized free-matrix-based integral inequality for stability analysis of time-varying delay systems. Applied Mathematics and Computation 2019; 354: 1-8. doi: 10.1016/j.amc.2019.02.009

[46] Seuret A, Gouaisbaut F. Hierarchy of LMI conditions for the stability analysis of time-delay systems. Systems & Control Letters 2015; 81 (1): 1-7. doi: 10.1016/j.sysconle.2015.03.007

[47] Vyhlídal T, Zítek P. Mapping based algorithm for large-scale computation of quasi-polynomial zeros. IEEE Transactions on Automatic Control 2009; 54 (1): 171-177. doi: 10.1109/TAC.2008.2008345

[48] Kammer AS, Olgac N. Delayed-feedback vibration absorbers to enhance energy harvesting. Journal of Sound and Vibration 2016; 363: 54–67. doi: 10.1016/j.jsv.2015.10.030

[49] Yuan C, Song S, Gao Q, Karimi HR, Pekař L et al. A novel frequency-domain approach for the exact range of imaginary spectra and the stability analysis of LTI systems with two delays. IEEE Access 2020; 8: 36595-36601. doi: 10.1109/ACCESS.2020.2973834

Appendix

The parameters and state variables of the two-area LFC system with DR given in Figure 1 are described in the following.

Table 4. Nomenclatures.

i	i^{th} area $(i = 1, 2, ..., n)$
Δf_i	Frequency deviation
ΔP_{Li}	Load disturbance
ΔP_{gi}	Power output of generator
ΔP_{mi}	Mechanical power output
ΔX_{gi}	Valve position
ΔP_{DRi}	Power output of DR control
D_i	Load damping coefficient
M_i	Inertia constant of generator
R_i	Governor speed drop characteristic
β_i	Frequency bias factor
F_{pi}	Total turbine power fraction
T_{ci}	Turbine time constant
T_{ri}	Reheater time constant
T_{gi}	Governor time constant
K_{Pi}, K_{Ii}	PI controller gains for both DR and LFC controller
α_{0i}, α_{1i}	Power sharing factors of generators and DR control loop
T_{12}	Tie-line synchronizing coefficient
τ_i	Time-delay
$\tau*$	Stability delay margin
ω_c	Crossing frequency

The coefficients of the augmented polynomial of (7):

$b_{15} = p_{15}T^2; b_{14} = p_{14}T^2 + 2p_{15}T; b_{13} = p_{13}T^2 + 2p_{14}T + p_{15};$

$b_{12} = (p_{12} - q_{12})\,T^2 + 2p_{13}T + p_{14}; b_{11} = (p_{11} - q_{11})\,T^2 + 2p_{12}T + p_{12};$

$b_{10} = (p_{10} - q_{10})\,T^2 + 2p_{11}T + p_{12} + q_{12}; b_9 = (p_9 - q_9 + r_9)\,T^2 + 2p_{10}T + p_{11} + q_{11};$

$b_8 = (p_8 - q_8 + r_8)\,T^2 + 2\,(p_9 - r_9)\,T + p_{10} + q_{10}; b_7 = (p_7 - q_7 + r_7)\,T^2 + 2\,(p_8 - r_8)\,T + p_9 + q_9 + r_9;$

$b_6 = (p_6 - q_6 + r_6)\,T^2 + 2\,(p_7 - r_7)\,T + p_8 + q_8 + r_8; b_5 = (p_5 - q_5 + r_5)\,T^2 + 2\,(p_6 - r_6)\,T + p_7 + q_7 + r_7;$

$b_4 = (-q_4 + r_4)\,T^2 + 2\,(p_5 - r_5)\,T + p_6 + q_6 + r_6; b_3 = -2r_4T + p_5 + q_5 + r_5; b_2 = q_4 + r_4\,.$

The coefficients of the augmented polynomial of (7) used in Step 2:

$b_{15} = T^2; b_{14} = 17.106T^2 + 2.0T; b_{13} = 110.34T^2 + 34.21T + 1.0; b_{12} = 329.98T^2 + 220.68T + 17.106;$

$b_{11} = 449.913T^2 + 667.91T + 110.34; b_{10} = 240.05T^2 + 976.85T + 337.93; b_9 = 68.54T^2 + 707.54T + 526.93;$

$b_8 = -8.2T^2 + 374.29T + 467.48; b_7 = -7.239T^2 + 96T + 467.48; b_6 = -1.527T^2 + 8.229T + 139.95;$

$b_5 = 0.295T^2 - 4.961T + 46.18; b_4 = 0.0206T^2 - 1.015T + 8.719; b_3 = -0.0425T + 0.736; b_2 = 0.0219\,.$